

## **NEAR FIELD SEISMIC RESPONSE OF STEEL MOMENT RESISTING FRAME RETROFITTED WITH PASSIVE FRICTION ENERGY DISSIPATING SYSTEMS**

Robert Tremblay\*, Andre Filiatrault\*\* and Spyridon Kremmidas\*\*\*

\*Associate Professor      \*\*\*Graduate Research Assistant  
EPICENTRE Research Group, Ecole Polytechnique

P.O. Box 6079, Station Centre-ville, Montreal, Quebec, Canada, H3C 3A7

\*\*Professor, Division of Structural Engineering, University of California at San Diego  
9500 Gilman Drive, Mail Code 0085, La Jolla, CA 92093, USA

### **ABSTRACT**

The performance of two passive friction damping systems for retrofitting steel moment-resisting frames is evaluated. Nonlinear dynamic analyses were performed on a six-storey moment-resisting frame designed according to current code provisions for California. The structure was subjected to three different earthquake ensembles. The first ensemble includes six near field records developed for major crustal earthquakes in California. The five records of the second ensemble are representative of near-field conditions in Los Angeles with a probability of exceedence of 10 % in 50 years. Finally, the third ensemble contains two far-field historical records.

Both friction systems are part of a steel chevron-bracing configuration used to retrofit the moment-resisting frame. In the first system, slotted-bolted connections that slip at a predetermined load are provided at one end of the bracing members. The second system includes double-acting ring-spring friction devices installed at the same locations. The main feature of the ring-spring system is a bi-linear hysteresis with a re-centering force that develops upon unloading and contributes in limiting permanent deformations. The slip load of the devices was determined based on a proposed procedure that takes into account the frequency content of the ground motions and the dynamic properties of the structure with and without the added bracing system.

**KEYWORDS:** Damping, Earthquake, Friction, Near Field, Ring-Spring, Steel Frames

### **INTRODUCTION**

Several steel moment-resisting framed buildings were seriously damaged as a result of the January 17, 1994 Northridge, California earthquake. Brittle weld fractures in beam-column connections occurred in the majority of these damaged buildings because of excessive curvature ductility demands. Although many investigations have led to the development of traditional retrofit strategies to reduce the curvature ductility demand in welded beam-column connections (haunched plates, reduced beam sections, etc.), little attention has been devoted to the use of friction passive energy dissipating devices, such as slotted-bolted friction dampers and ring-spring devices. As shown by the large array of recorded ground motions during the Northridge earthquake, buildings in Southern California must sustain short duration, impulse-type, base excitation. It is not clear how supplemental damping systems, such as friction devices, would perform under such impulsive seismic input.

To shed some light on this question, this paper investigates the performance of the two passive energy dissipating systems described above for the retrofit of a six-storey moment-resisting frame subjected to three different ensembles of strong ground motions. Two of those ensembles are representative of near-field conditions in the Los Angeles area. The third ensemble includes two historical records that have been extensively used in past research. The slip load of the energy dissipating devices was determined based on a proposed procedure that takes into account the frequency content of the ground motions and the dynamic properties of the structure with and without the added bracing system.

## DESCRIPTION OF BUILDING STRUCTURE AND RETROFIT SYSTEMS

The six-storey building structure analyzed herein was studied by Tsai and Popov (1988) and was modified by Hall (1995). As shown in Figure 1, the building is rectangular in shape and is braced in the North-South direction by two exterior moment-resisting frames. The design complies with the 1994 UBC code requirements (ICBO 1994) for a building located in Zone 4 on soil type S2. Design gravity loads included the roof dead load (3.8 kPa), the floor dead load (4.5 kPa), the roof live load (1.0 kPa), the floor live load (3.8 kPa), and the weight of the exterior cladding (1.7 kPa). Wind loads were based assuming a basic wind speed of 113 km/h and an exposure type B. The steel grade is assumed to be A36 (nominal  $F_y = 248$  MPa) for all members.

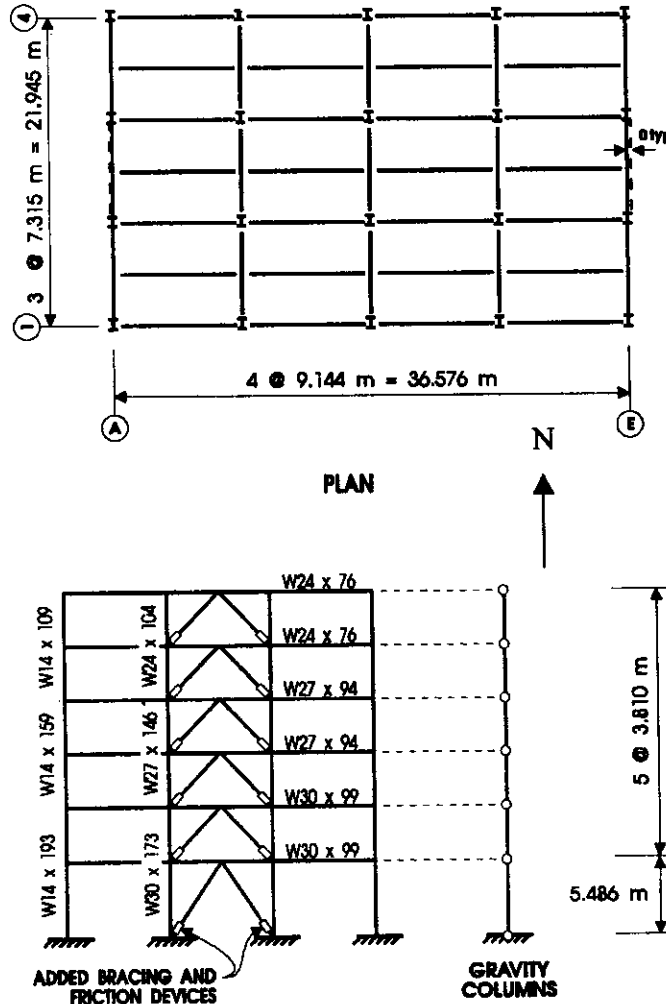


Fig. 1 Building studied

The retrofit strategy for the structure consisted of introducing a chevron braced frame in the middle bay of each moment resisting frame and installing passive energy dissipating devices at one end of the bracing members, as shown in Figure 1. The bracing members were designed to sustain the greater of the forces due to wind and floor live loads and the slip load assigned to the device. Brace forces induced by dead loads were ignored in the design of the bracing and friction energy dissipating systems, as it was assumed that the braces would be installed after the building would be completed.

The first retrofit system considered incorporates at one end of the bracing members slotted-bolted connections that slip at a predetermined load. This system exhibits the well-known rigid-plastic hysteretic behaviour shown in Figure 2. This hysteretic behaviour can be achieved by various friction surfaces and mechanical configurations (Grigorian and Popov 1993; Pall and Marsh 1982; Tremblay and Stierner 1993).

The second retrofit system consists of double-acting ring-spring friction devices installed between the braces and the steel frame. As illustrated in Figure 2, the main feature of the ring-spring system is a super-elastic behaviour characterized by a bi-linear hysteresis with a re-centring force that develops upon unloading and contributes in limiting permanent deformations (Kar et al. 1998, Kar et al. 1996, Kar and Rainer 1995, 1996, Shepherd and Erasmus 1988).

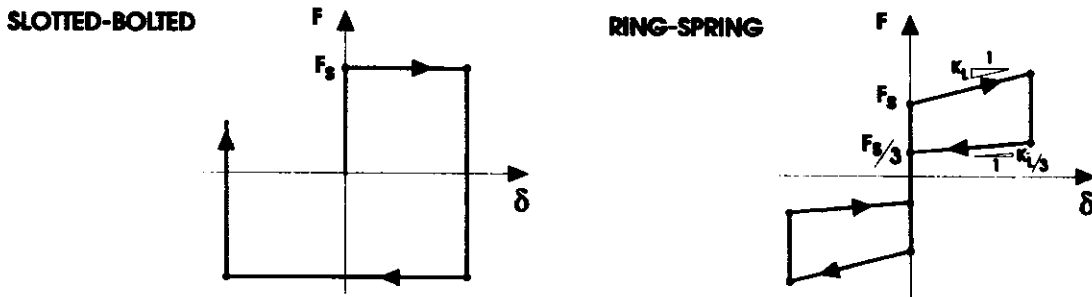


Fig. 2 Hysteretic behaviour of energy dissipating systems

## DESIGN OF ENERGY DISSIPATING SYSTEMS

### 1. Slotted-Bolted Connections

The only parameter to be determined for the slotted-bolted system is the slip load of each device along the building height. Earlier numerical studies (Filiatrault and Cherry, 1988) have indicated the feasibility of using an optimum slip-shear distribution that is proportional to the inter-storey drift arising from a first mode vibration of the structure. For the building structure considered in this study, the slip shear,  $V_{si}$ , at a given storey  $i$ , is related to the slip load of each device,  $F_{si}$ , by:

$$V_{si} = 2F_{si} \cos \alpha_i \tag{1}$$

where  $\alpha_i$  is the angle of inclination from the horizontal of the braces in the storey  $i$ .

It has been shown (Filiatrault and Cherry, 1988), however, that very little benefit is achieved from the use of this optimum distribution as compared with the use of the simpler uniform slip shear distribution. Therefore, the slip shear was assumed constant for each storey of the building structure investigated in this study.

The common optimum slip load was determined based on a proposed procedure that takes into account the frequency content of the ground motion and the dynamic properties of the structure with and without the added bracing system (Filiatrault and Cherry 1990). For a given ground motion, the optimum slip load is determined by minimizing a Relative Performance Index ( $RPI$ ) derived from energy concepts:

$$RPI = \frac{1}{2} \left[ \frac{SEA}{SEA_0} + \frac{U_{max}}{U_{max0}} \right] \tag{2}$$

where  $SEA$  is the strain energy area, i.e., the area under the elastic strain energy time-history for all structural members of a friction damped structure,  $SEA_0$  is the strain energy area for a zero slip load,  $U_{max}$  is the maximum value of the elastic strain energy stored in all structural members of a friction damped structure and  $U_{max0}$  is the maximum elastic strain energy for a zero slip load.

Values of the Relative Performance Index ( $RPI$ ) are such that:

- $RPI = 1$ , the response corresponds to the behaviour of an unbraced structure (slip load = 0);
- $RPI < 1$ , the response of the friction damped structure is "smaller" than the response of the unbraced structure;

$RPI > 1$ , the response of the friction damped structure is "larger" than the response of the unbraced structure.

In order to determine the optimum slip load that minimizes the  $RPI$  value for a given ground motion, a stream-line computer program called FDBFAP (Filiatrault and Cherry 1990) was created. This program computes the  $RPI$  values for a given range of physically admissible slip loads. From the results of a parametric study with this program and artificially generated ground motions, a general design procedure has been proposed to evaluate the optimum slip load of a structure located at a given site.

This procedure recommends the selection of diagonal cross braces such that:

$$T_b / T_u < 0.40 \quad (3)$$

where  $T_u$  is the fundamental period of the unbraced structure and  $T_b$  is the fundamental period of the braced structure. It was found that the best response (minimum  $RPI$ ) of friction damped structures occurs for small values of  $T_b / T_u$ , which corresponds to large diagonal cross-braces. Therefore the diagonal cross-braces should be chosen with the largest possible cross-sectional area within the limits of cost and availability of material.

For the structure considered herein,  $T_u = 1.304$  s and with a choice of the largest hollow steel section readily available (HSS 12 × 12 × 5/8):  $T_b = 0.648$  s. Therefore:  $T_b / T_u = 0.497$  in this case.

The procedure then requires the evaluation of the peak ground acceleration,  $a_g$ , and the predominant ground period,  $T_g$ , for the construction site. In this study, a value of  $a_g = 0.40$  g, corresponding to the Z factor for zone 4 in the UBC code (ICBO 1994), was retained. Also, a value of  $T_g = 0.4$  s was assumed as it corresponds to the predominant period of simulated ground motions for the Los Angeles region (SAC Joint Venture 1995).

From these parameters, a design slip load spectrum can be constructed to estimate the total slip shear,  $V_0$ , of the structure (Filiatrault and Cherry, 1990). This design slip load spectrum allows the determination of an equivalent seismic coefficient to evaluate the total slip shear  $V_0$ . For the structure considered in this study, we find:

$$V_0 = 0.863 \frac{a_g}{g} W = (0.863)(0.4)(28950 \text{ kN}) = 9994 \text{ kN} \quad (4)$$

where  $W$  is the total seismic weight of the structure (28950 kN) and  $g$  is the acceleration of gravity.

The total slip shear is distributed uniformly among the bracing at each floor of the two exterior frames:

$$V_{ii} = \left( \frac{1}{2} \right) \left( \frac{9994}{6} \right) = 830 \text{ kN} \quad (5)$$

Using Equation (1), the optimum slip load for each of the two dampers located in the first storey is given by:

$$F_{s1} = \frac{830 \text{ kN}}{2 \cos 56.3^\circ} = 750 \text{ kN} \quad (6)$$

The optimum slip for each damper in all other storeys is given by:

$$F_{si} = \frac{830 \text{ kN}}{2 \cos 46.2^\circ} = 600 \text{ kN}, \quad i = 2 \text{ to } 6 \quad (7)$$

Several assumptions that were made in the development of this procedure may not be representative of the conditions that would prevail in a severe earthquake occurring in the vicinity of a populated area along the west coast of the United States. For instance, the response of the structure was assumed to remain essentially elastic under the ground motions, and the artificially-generated ground motions that were used to develop the design slip load spectrum did not contain any damageable severe acceleration pulses that are expected in the near-field of major earthquake events. In addition, the choice of the two

parameters ( $SEA$  and  $U_{max}$ ) may not be appropriate to minimize structural and non-structural damage in actual buildings. Other parameters such as peak inter-storey drifts or floor absolute accelerations are now commonly used to evaluate the seismic performance of a structure. These aspects are investigated in this study by examining the performance of the building considered under severe ground motion conditions that are expected in the Los Angeles area.

## 2. Ring-Spring System

As illustrated in Figure 2, each ring-spring device is characterized by two parameters: a slip force,  $F_s$ , and a loading slip stiffness,  $K_L$ . For actual device prototypes, the unloading slip stiffness and the residual re-centring force are a ratio of the loading slip stiffness and of the slip load, respectively. A typical value of 1/3 was assumed for this ratio.

No procedure currently exists to optimize the physical parameters of a ring-spring system. In this study, for comparison purposes, the parameters of the ring-spring system were derived from the parameters of the slotted-bolted devices described earlier. With this procedure, the effect of the re-centring capabilities of the ring-spring system on the structural response could be isolated. The slip load of each ring-spring device was made equal to the slip load of the corresponding slotted-bolted friction device. A small loading stiffness,  $K_L$ , corresponding to 0.16 % of the axial stiffness of the bracing members was introduced in each ring-spring device to counter the apparent loss of lateral stiffness caused by P-delta effects on the structure.

## CHOICE OF EARTHQUAKE GROUND MOTIONS

The structure was subjected to three ensembles of ground motions. The first set, referred to as NF, includes six near-fault motions on firm ground that were selected from a suite of time histories that had been developed for major crustal earthquakes in UBC Seismic Zone 4 (SAC Joint Venture 1997). Such short duration, impulsive type of ground motions are typical for M6.75 – M7.5 earthquakes at a distance less than 18 km. These ranges dominate the seismic risk for a probability of exceedence of 10 % in 50 years in Zone 4. In this group, only ground motion components perpendicular to the faulting mechanism were retained as their amplitude was higher. Ground motion time histories of the second ensemble (LA) were selected from a suite of historical recordings from M6 – M7.3 range earthquakes which were scaled to match the 10 % probability of exceedence in 50 years uniform hazard spectrum for Los Angeles (SAC Joint Venture 1997).

For these two ensembles of ground motions, accelerograms that exhibited either one or more of the following characteristics were selected: high spectral acceleration peak at any period, high spectral acceleration at a period corresponding to the fundamental period of the braced frame,  $T_{1B} = 0.648$  s, high spectral acceleration at the fundamental period of the unbraced frame,  $T_{1U} = 1.304$  s, high ratio of the spectral accelerations at  $T_{1B}$  and at  $T_{1U}$ , and low ratio of the spectral accelerations at  $T_{1B}$  and at  $T_{1U}$ . The 5 % damping spectral characteristics of the selected ground motions are given in Table 1.

The third group of ground motions included the unscaled S00E El Centro record from the 1940 Imperial Valley Earthquake and the S69E Taft Lincoln Tunnel record from the 1952 Kern County Earthquake. These two ground motions have been used extensively in past studies and are considered herein as a reference for comparison purposes.

The acceleration time-histories and the absolute acceleration response spectra at 5 % damping for all ground motions considered are shown in Figures 3 and 4, respectively. When compared to the LA ground motions, the NF records generally are of higher amplitude, release their energy within a few strong pulses and exhibit a longer dominant period. The El Centro and Taft records have a frequency content similar to the LA ground motions but their amplitude is significantly lower. Note that the LA02 accelerogram is the S00E El Centro record scaled up by a factor of 2.0.

## MODELLING ASSUMPTIONS

The analyses were performed using the RUAUMOKO nonlinear dynamic analysis program (Carr 1996). Only half of the building was modelled as the structure is symmetrical. As shown in Figure 1, the

model then included only one exterior frame, together with one gravity column that represents all interior frame columns. The total gravity loads acting on the interior columns were applied to the gravity column in the model and both the gravity column and the exterior frame were constrained to experience the same lateral deformation at each floor.

Only the bare steel frame was included in the analyses, i.e., the slab participation as composite beams was not included. The inelastic response was concentrated in plastic hinges that could form at both ends of the frame members. These plastic hinges were assigned a bi-linear hysteretic behaviour with a curvature strain hardening ratio of 0.02, and their length was set equal to 90 % of the associated member depth. The plastic resistance at the hinges was based on an expected yield strength of 290 MPa. An axial load-moment interaction, as per LRFD 1993 (AISC 1993), was considered for the columns of the structure. Rigid-end offsets were specified at the end of the frame members to account for the actual size of the members at the joints. The panel zones of the beam-column connections were assumed to be stiff and strong enough to avoid any panel shear deformation and yielding under strong earthquakes. This assumption represented the most critical condition for the inelastic curvature demand on the welded beam-to-column joints, as all the hysteretic energy must be dissipated only through plastic hinging in the beams and the columns. The columns were fixed at the ground level, except the gravity column which was assumed pinned at the base and at each level.

Gravity loads acting on the frame during the earthquake were assumed equal to the roof and floor dead loads, the weight of the exterior walls, and a portion of the floor live load (0.7 kPa). P-delta effects were accounted for in the analyses, including P-delta forces generated in the interior frames. Half the weight of the building, along with a 0.5 kPa live load, was included in the reactive weights at each level. Rayleigh damping of 5 % based on the first two elastic modes of vibration of the structure was assigned. Each analysis was performed at a time-step increment of 0.002 s.

**Table 1: Absolute Spectral Accelerations of Ground Motions**

Ground motion	$S_a$ (g)			$S_a$ at $T_{1B}$ $S_a$ at $T_{1U}$
	Maximum	at $T_{1B} = 0.648$ s	at $T_{1U} = 1.304$ s	
NF03	3.15	2.83	1.13	2.50
NF17	3.78	2.55	1.36	1.88
NF19	2.80	1.32	2.69	0.49
NF23	5.21	3.15	4.53	0.70
NF27	3.00	3.00	1.93	1.55
NF29	3.62	2.28	2.20	1.04
LA02	1.78	1.36	0.45	3.02
LA09	1.25	1.20	1.13	1.06
LA12	3.60	1.03	0.23	4.48
LA14	2.40	2.00	0.90	2.22
LA18	2.78	1.42	0.81	1.75

## NUMERICAL RESULTS FOR SLOTTED BOLTED SYSTEM

In this section, the behaviour of the structure retrofitted with the slotted bolted system under all three ensembles of ground motions is compared to that of the original bare steel frame without the energy dissipating system. The response parameters of interest are the inter-storey drift, the absolute floor horizontal acceleration, and the inelastic demand in the beams and the columns. The influence of the slip load on these parameters is examined first. Thereafter, the effects of varying the stiffness of the bracing members and the vertical distribution of the slip load are investigated.

### 1. Peak Inter-Storey Drifts

Inter-storey drift is an indicator of both structural and non-structural damage. For instance, the Vision 2000 document (SEAOC, 1996) suggests that a building is operational with light damage if the inter-storey drift is less than 0.5 % and that structural damage is expected to develop at an inter-storey drift of 1.5 %. Figures 5 and 6 present the peak inter-storey drift-slip shear relationship computed at every floor

of the building studied under the NF and LA ground motion ensembles, respectively. The results obtained under the El Centro and Taft records are also shown in both figures for comparison purposes.

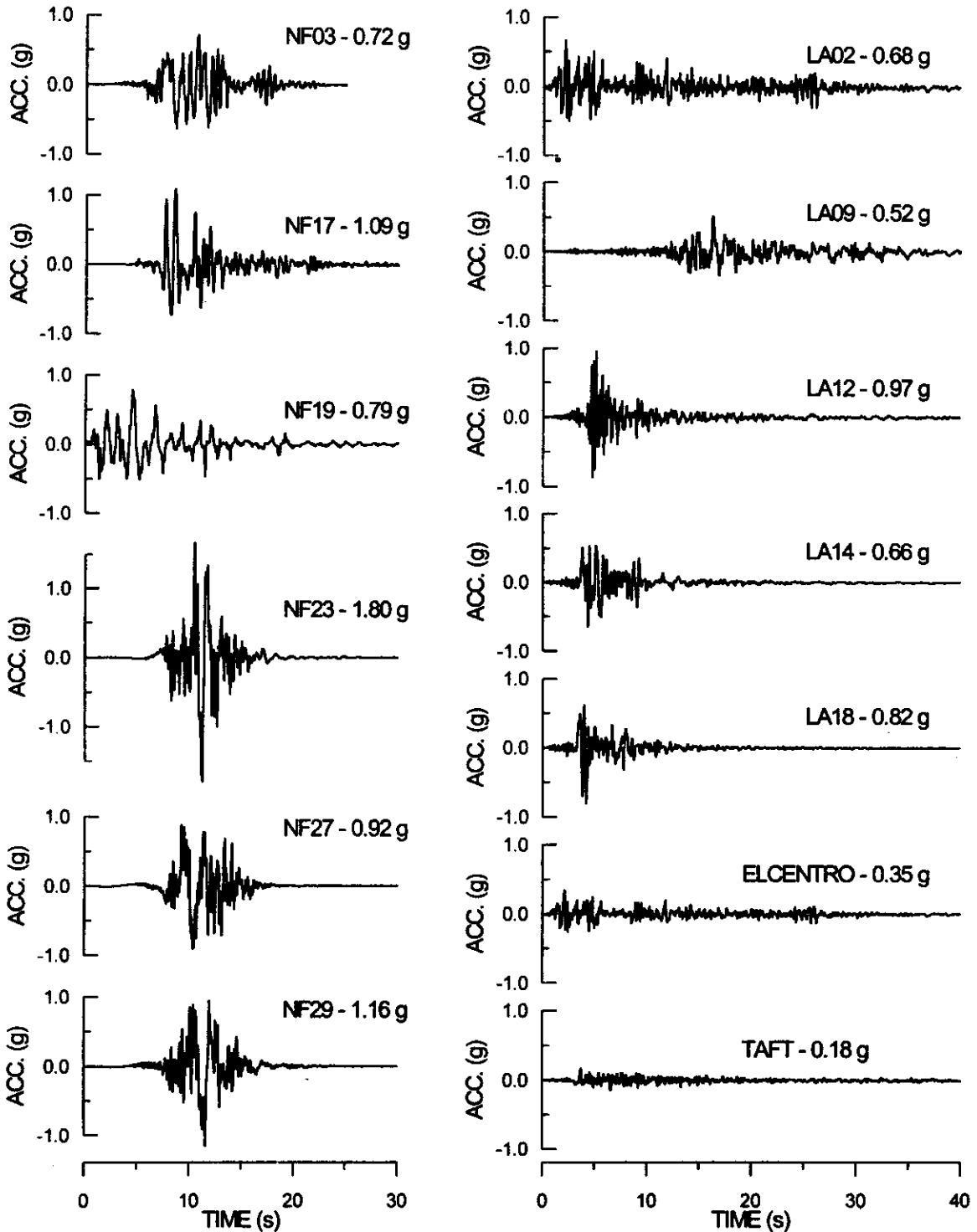


Fig. 3 Time histories of earthquake ground motions

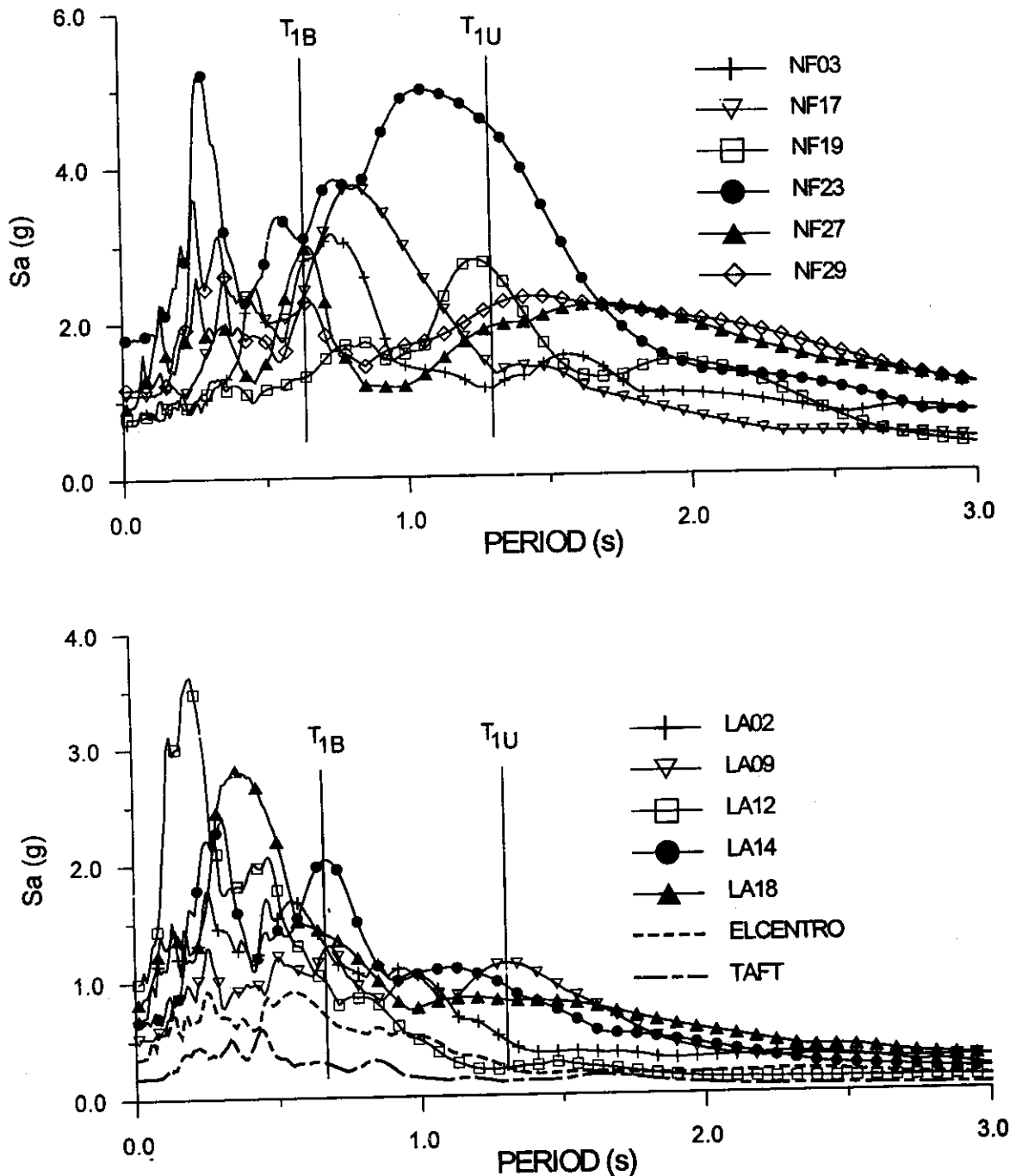


Fig. 4 Response spectra of earthquake ground motions

In general, the building equipped with the slotted-bolted system experienced smaller deformations than the unbraced frame ( $V_{si} = 0$ ) but the response varies with the level. For the three upper floors, we note that i) all ground motion records within a given ensemble produce similar effects, ii) the reduction in storey-drift due to the addition of the slotted-bolted system is very significant for all three groups of ground motions, iii) the performance of the system under the NF and LA ground motions is nearly identical, iv) the amplitude of the deformations is within acceptable limits, and v) there is a clear optimum slip shear that minimizes the inter-storey drift. In addition, the optimum slip shear as predicted by the procedure described earlier ( $V_{si} = 830$  kN) nearly corresponds to that obtained from the analyses for the LA and NF ground motions. For the El Centro and the Taft records, the optimum slip shear is



approximately half the predicted value. This is expected since these two records exhibit peak accelerations much lower than the NF and LA ground motions, and the computed optimum slip shear is linearly proportional to the peak ground acceleration (Equation (4)).

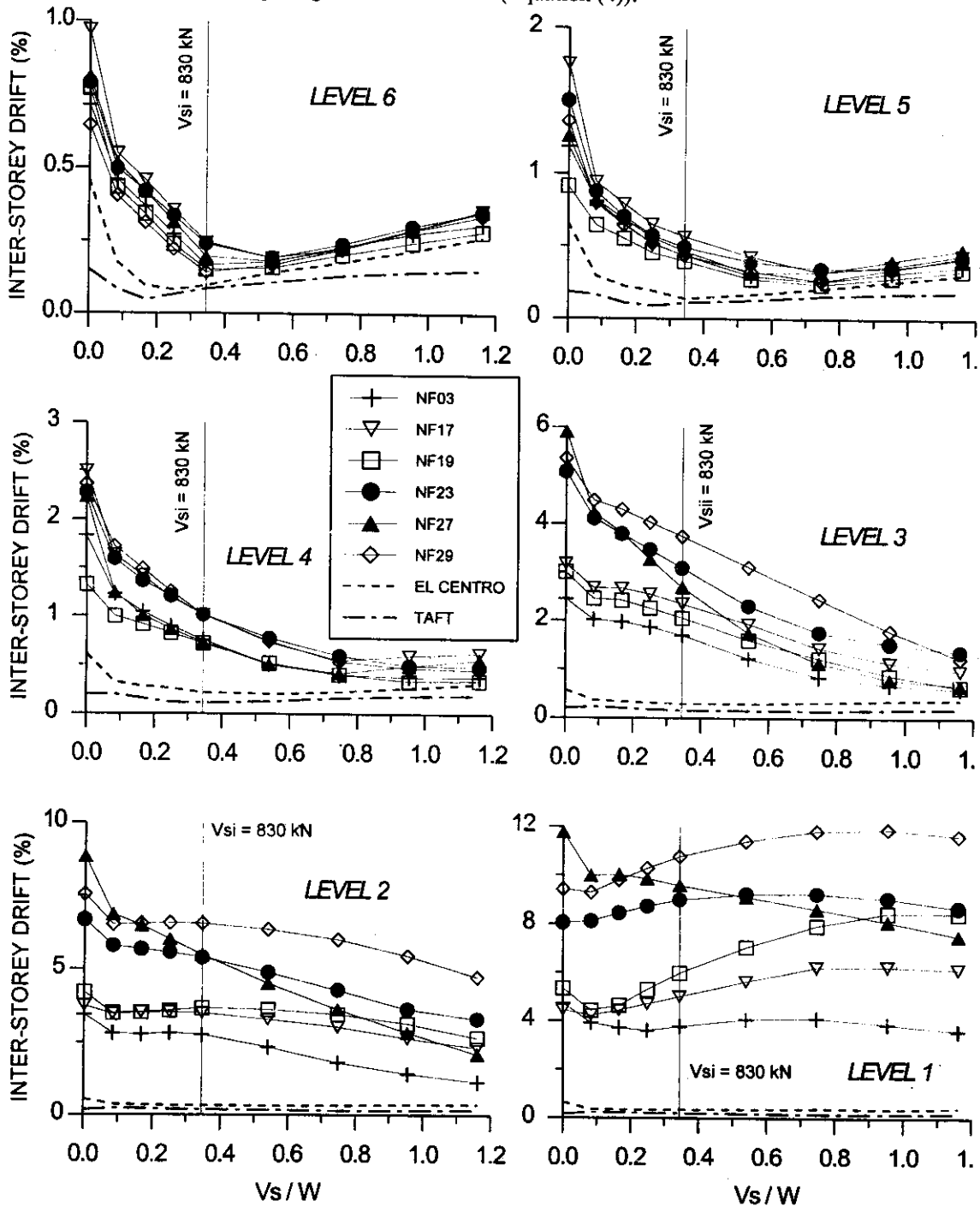


Fig. 5 Peak inter-storey drifts, slotted bolted system, near-fault (NF) ground motions

As we go down the building, the results become more scattered for each group of ground motions. The inter-storey drifts also generally increase, the performance of the system becomes less remarkable, especially under the NF records, and the optimum slip shear is less defined. Under the El Centro and the Taft records, the proposed  $V_{si} = 830$  kN still appears to be an effective solution as the associated inter-storey drift is kept below 0.5% at every floor and does not decrease significantly if a higher slip load is

specified. Overall, an 830 kN slip shear also gives satisfactory results under the LA motions, with peak inter-storey drifts remaining within 2 % of the storey height. A higher slip load would have permitted to reduce further the deformations at levels 2 and 3, however, and it can also be noticed that the addition of the slotted-bolted system was not successful in reducing the storey drift at the bottom floor under the LA14 and LA18 records. When subjected to the NF ground motions, the results indicate that adding a slotted-bolted system with realistic slip shear is not sufficient to guard against excessive inter-storey drifts in the lower floors of the building. At the bottom floor, the response with high slip load under most NF records is even more critical than that of the original unbraced frame.

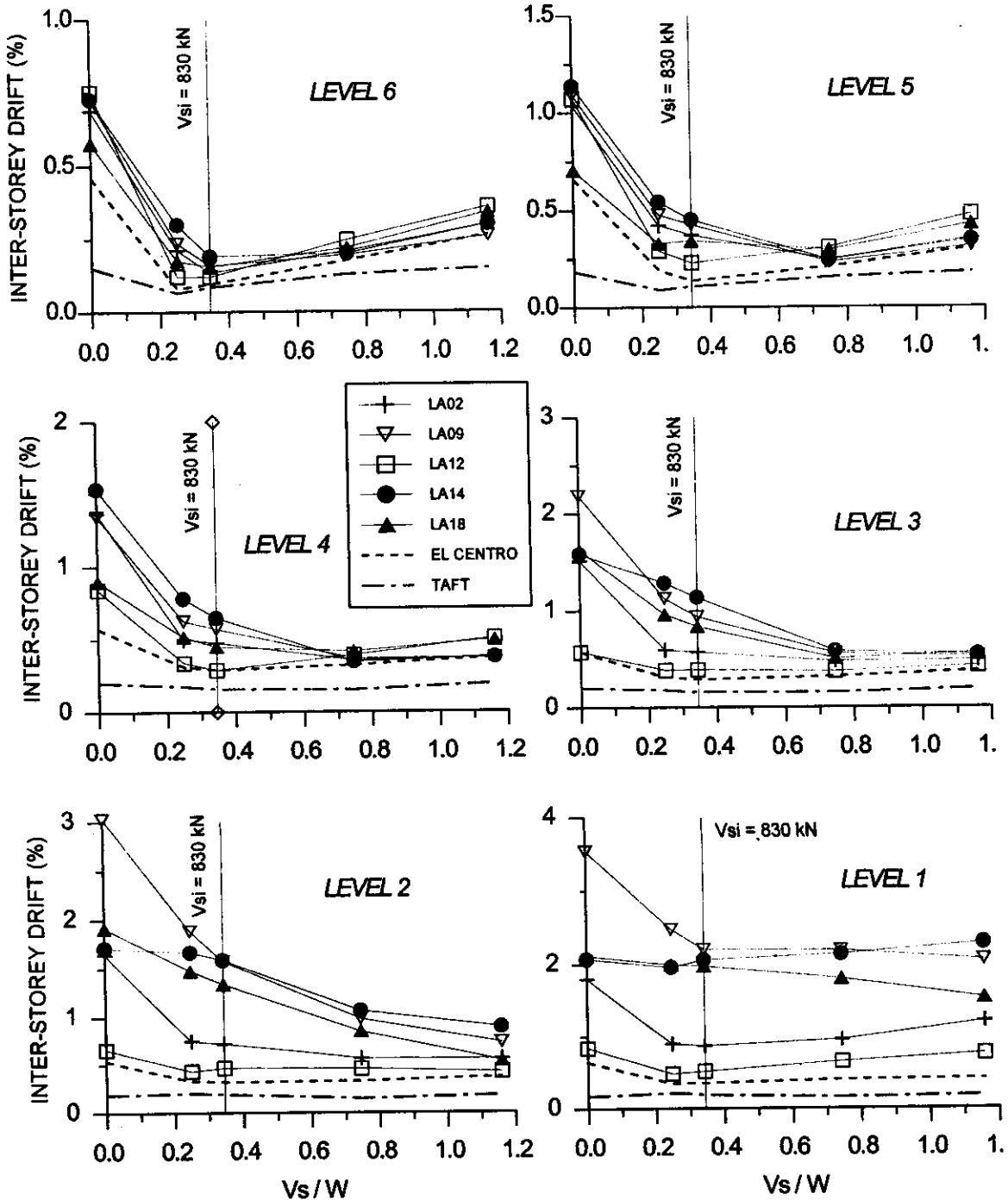


Fig. 6 Peak inter-storey drifts, slotted bolted system, LA ground motions

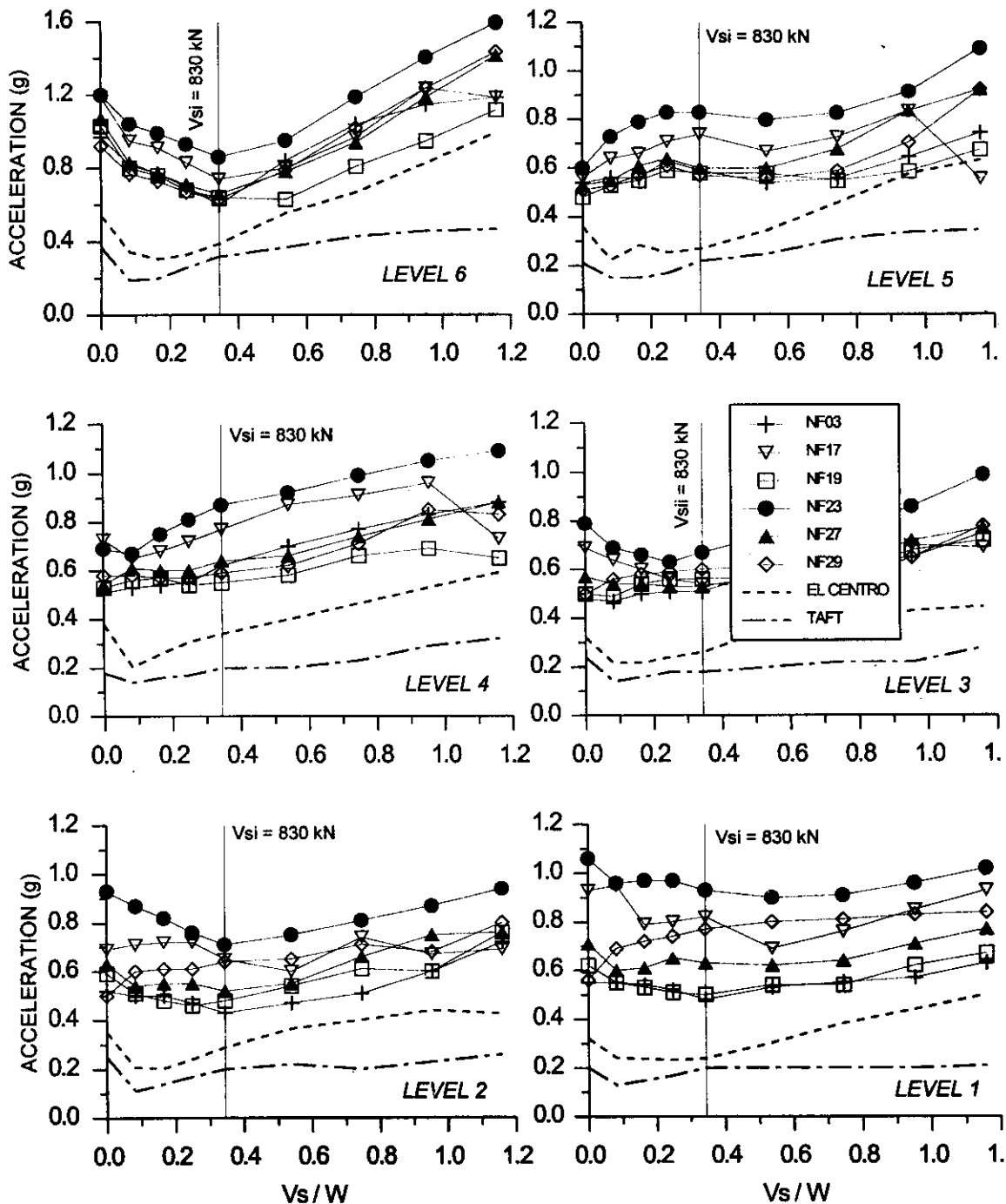


Fig. 7 Peak absolute floor accelerations, slotted bolted system, near-fault (NF) ground motions

The difference in performance under the NF ground motions is most likely due to the impulsive nature of these ground motions. The large inter-storey drifts at the bottom floors developed during large acceleration pulses which fed energy in the structure as it deforms unidirectionally, before the building starts to oscillate. Under the more stationary LA ground motions and the El Centro and Taft records, the system is more efficient in reducing the dynamic response of the structure.

## 2. Peak Absolute Floor Accelerations

Horizontal inertia forces that develop at each level of a building are proportional to the absolute horizontal accelerations experienced by the building and this parameter is therefore important to assess

the performance of non-structural elements such as ceilings, attachments for mechanical equipment, shelves, office furniture, etc. Figure 7 and 8 give the peak absolute acceleration-slip shear relationship computed at every floor of the building studied under the different ground motions.

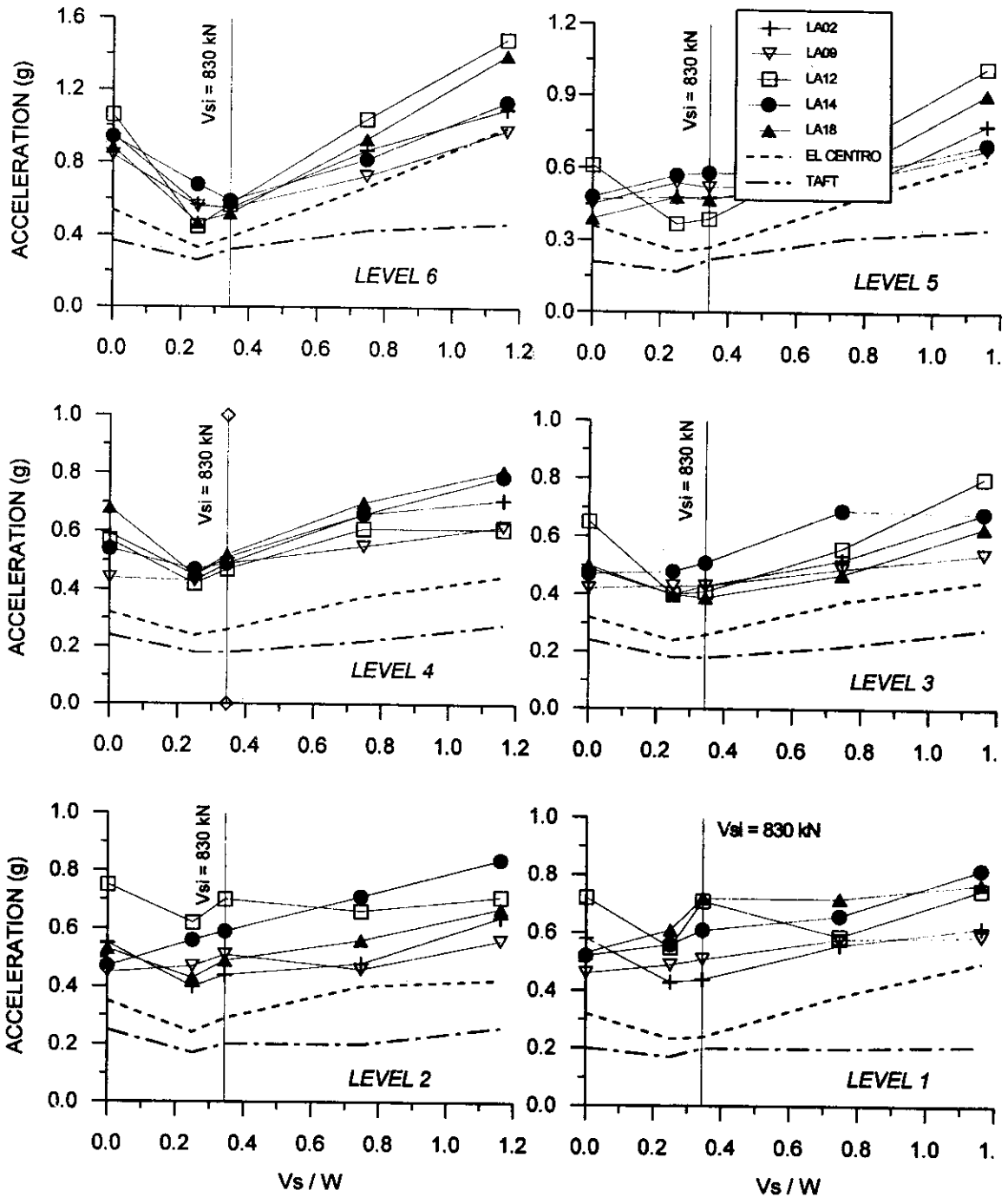


Fig. 8 Peak absolute floor accelerations, slotted bolted system, LA ground motions

Again, the response varies with the level in the building. At the top floor, the behaviour is similar to that observed for the inter-storey drift: all ground motions of the same group have similar effects and, for each accelerogram ensemble, there exists an optimum slip shear to which corresponds minimum peak acceleration. For the El Centro and Taft records, this optimum is again approximately equal to half the predicted value of 830 kN. For the LA and NF ensembles, the predicted optimum slip shear matches closely the results of the analyses.

Under the El Centro and Taft records, the efficiency of the slotted-bolted system at the lower floors is maintained as the peak accelerations at  $V_{si} = 415$  kN are lower than in the unbraced frame and correspond to, or are close to, the minimum values. Interestingly, the minimum peak acceleration under these two ground motions is very similar from one floor to another. Under the NF ground motions, the computed peak accelerations at levels 1 to 5 remain approximately constant or even increase as the slip shear is increased. Only at level 2, does the peak absolute acceleration decrease near the proposed slip shear  $V_{si} = 830$  kN. This indicates that a passive friction system would not be effective in reducing non-structural damage in multi-storey structures subject to near-field ground shaking. Under the LA ground motions, the use of the slotted-bolted system permitted to reduce the accelerations in the third and fourth floors near  $V_{si} = 830$  kN. At the other levels, the accelerations are generally higher than in the unbraced frame, regardless of the slip shear considered.

### 3. Peak Inelastic Demand in Beams and Columns

The peak ductility demand in both beams and columns was generally observed at the first floor. Hence, only the maximum values computed in the first floor beams and at the bottom of the first storey columns are presented in Figures 9 and 10 for different amplitudes of the slip shear. In these figures, the inelastic demand is expressed as the maximum plastic rotation experienced in the plastic hinges. The limit of 0.03 radian adopted by the AISC design provisions (AISC 1997) for ductile steel moment resisting frames is shown on the graphs as a reference.

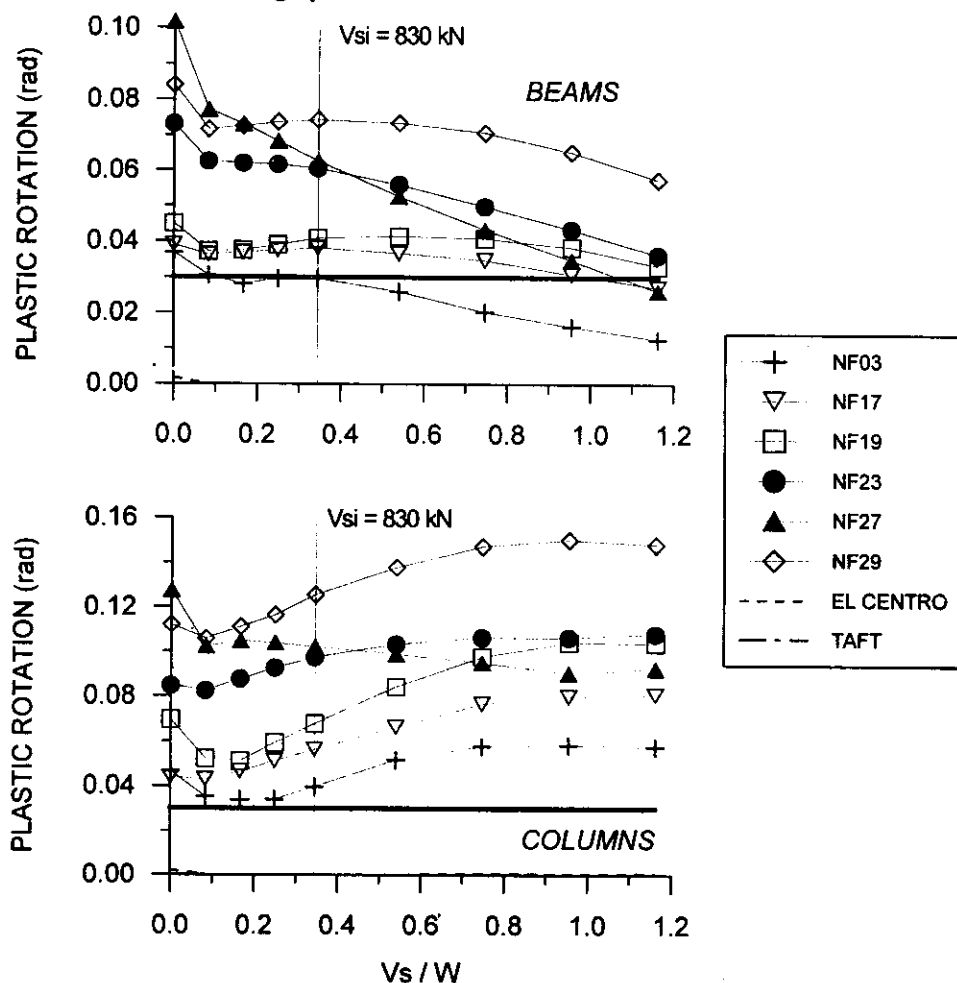


Fig. 9 Peak plastic rotations in first storey beams and columns, slotted bolted system, near-fault (NF) ground motions

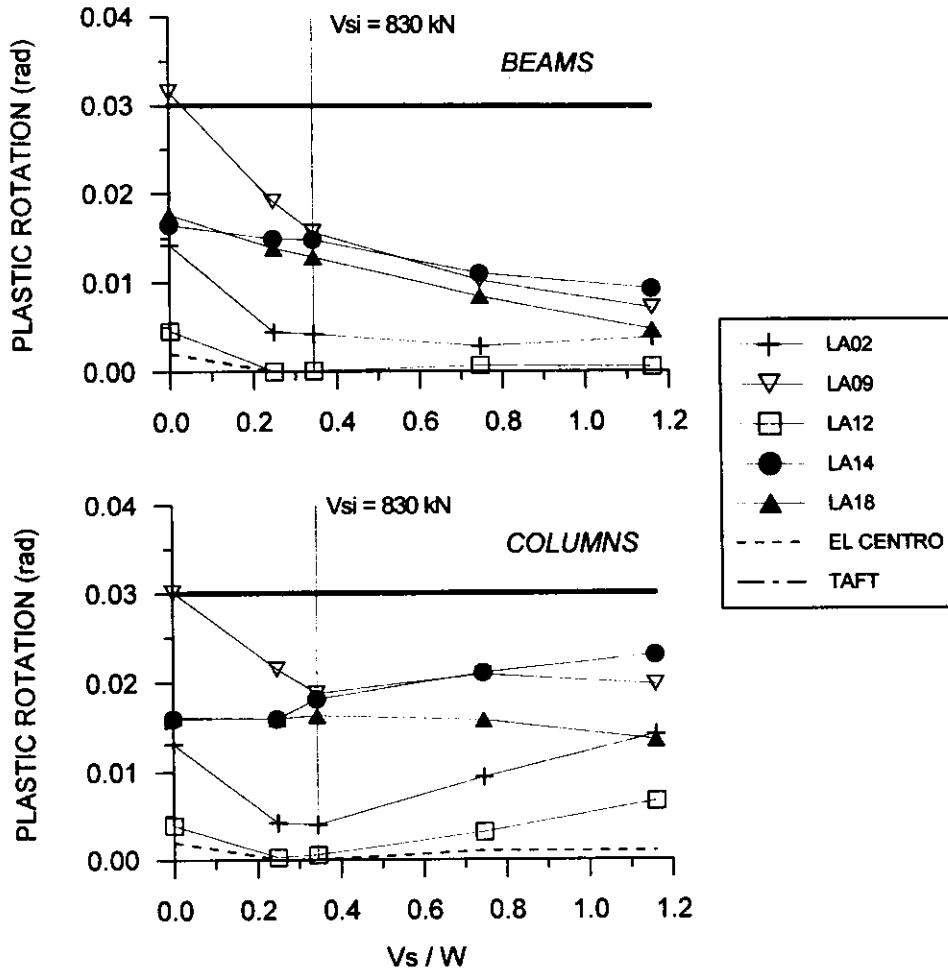


Fig. 10 Peak plastic rotations in first storey beams and columns, slotted bolted system, LA ground motions in: a) first floor beams; b) first floor columns

The response of the building remained essentially elastic under the El Centro and the Taft record, which corresponds to the assumption made in the development of the procedure by Filiatrault and Cherry (1990). This could explain why the addition of a passive friction energy dissipating system results, under these ground motions, in a behaviour similar to that predicted by these authors.

Under both the NF and LA ground motions, the unbraced frame experienced significant inelastic demand in the first floor members, well in excess of the 0.03 radian limit for the NF records. The demand in the beams generally reduces when the energy dissipating system is added to the unbraced frame, but there is no clear optimum slip shear where the inelastic demand is minimum. For the NF records, however, specifying realistic slip shear levels does not permit to reduce the inelastic rotation in the beam plastic hinges below the 0.03 radians limit for most ground motions. For both the NF and LA ground motions, the variation of the plastic demand with the slip shear is similar to the variation of the inter-storey drift at the first floor (Figures 5 and 6). This was expected as the plastic rotation at the base of the first storey columns of the building is related to the deformation of that storey. In the case of the NF records, the increase in column response for increasing slip shears is even more pronounced than the increase in the inter-storey drift, and the plastic rotational demand could not be reduced under the 0.03 radian limit.

#### 4. Influence of the Axial Stiffness of the Bracing Members

The building was analyzed under the NF03, NF17, and the NF23 ground motions to examine the influence of varying the axial stiffness of the bracing members. Two additional different stiffness levels were considered: half the original brace stiffness and twice the original brace stiffness. The slip shear was

maintained equal to  $V_{si} = 830$  kN. For all ground motions, the inter-storey drift and the ductility demand in both the beams and the columns were found to diminish when the stiffness was doubled. Conversely, these response parameters increased when more flexible bracing systems were specified. Typical variations are shown in Figure 11. This behaviour is in agreement with the findings of Filiatrault and Cherry (1990). It can be attributed to the fact that sliding of the energy dissipating devices is activated at lower deformation levels with stiffer braces, which makes the system more effective.

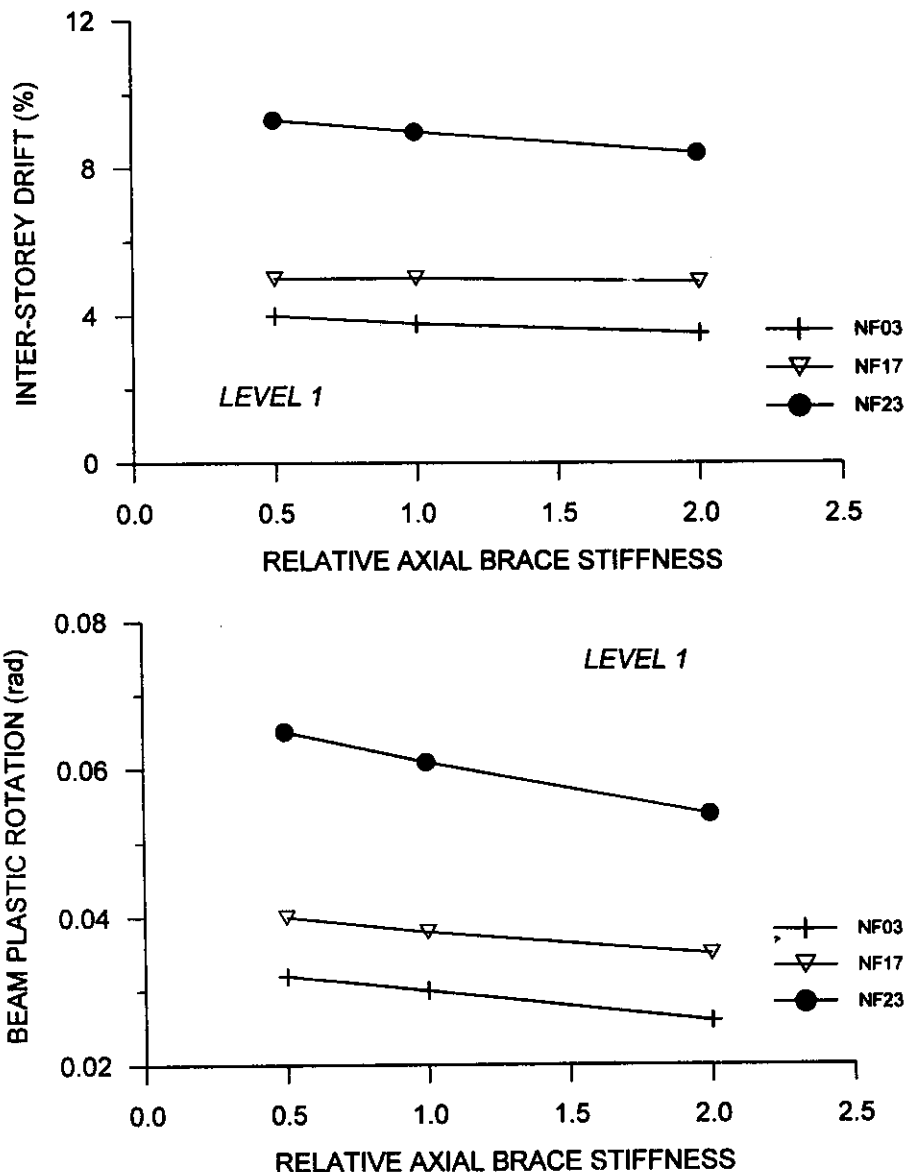


Fig. 11 Influence of the brace stiffness on the first inter-storey drift and on the maximum ductility demand in the first storey beams

### 5. Influence of the Vertical Distribution of the Slip Load

The building was also analyzed under the same three ground motions (NF03, NF17, and NF23) to investigate the influence of varying the vertical distribution of the slip load. The slip shear was set equal to 830 kN at the base of the building and was varied linearly towards the top in order to have an average slip shear of 600 kN over the height of the building. The results were compared to the response with a uniform slip shear  $V_{si} = 600$  kN. The same procedure was followed with  $V_{s1} = 2800$  kN and an average slip shear of 1800 kN.

Figure 12 shows for the results for both average shear slip loads. For each floor, the increase or the reduction in the peak inter-storey drift due to the use of a variable slip load is shown. For instance, a reduction of 1 % in the figure indicates that the inter-storey drift has decreased by 1 % of the storey height when using a variable slip load. As expected, the modification in the vertical slip load distribution results in a more uniform vertical distribution of the storey drift: the deformations in the upper floors are generally increased while those in the bottom storeys are reduced. However, the differences in inter-storey drift between the non-uniform and uniform slip shear cases are small, as already observed by Filiatrault and Cherry (1988), and the reduction in the lower floor deformations is not sufficient to reach an acceptable drift level of 2 % of the storey height. In design, one must also consider that the benefits of using a variable slip load can be offset by the associated greater complexity in both fabrication and installation.

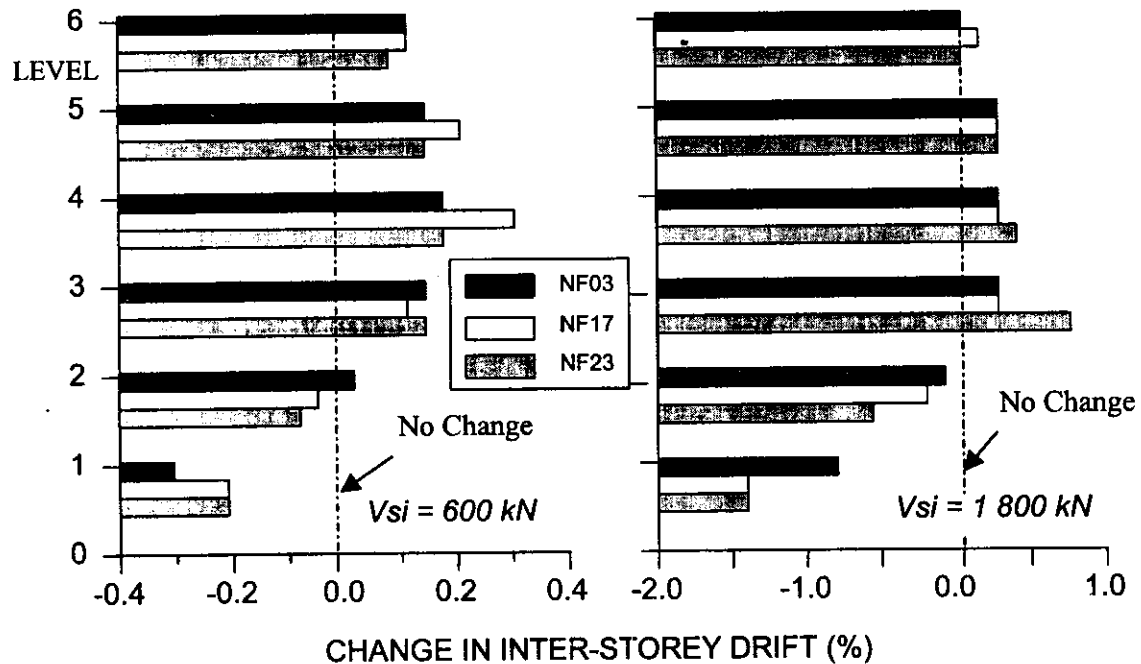


Fig. 12 Influence of the vertical distribution of slip load on the inter-storey drift

## RESULTS FOR RING-SPRING SYSTEM

For the ring-spring system, only the response under the LA14 and LA18 ground motions has been examined and compared to that of the slotted-bolted system. As shown in Table 1, these two ground motions exhibit the highest acceleration spectral ordinate for the LA group of records at a period corresponding to the period of the braced frame. In this investigation, the analyses were performed for the first 30 s of each ground motion, followed by 5 s of free vibrations to evaluate the residual deformations of the structure.

The plastic hinging distribution resulting from the analyses is shown in Figure 13. For each structural configuration, under each ground motion, the occurrence of a plastic hinge at the end of a frame member is indicated along with the maximum curvature ductility demand. Uni-directional and bi-directional yielding are also differentiated in the figure.

The ductility demand in the lower columns and beams of the unbraced structure is similar for both earthquake ground motions. Maximum curvature ductility demands of 6.3 and 6.5 occur at the base of the central columns under the LA14 and the LA18 ground motions, respectively. The corresponding maximum curvature ductility levels in the first floor beams of the structure are 6.5 and 6.9 corresponding to plastic rotations of 0.017 rad and 0.018 rad, respectively.

The two ground motions impose significantly different plastic hinging distributions in the upper beams and columns of the unbraced structure. The LA14 ground motion causes much more yielding in the upper members than the LA18 ground motion. These different yielding patterns in the upper levels



could be attributed to more significant higher mode contributions under the LA14 earthquake than under the LA18 ground motion (see Figure 4). The yielding patterns resulting from the two retrofit strategies are similar, however. The upper beams and columns remain in the elastic range of the steel with both retrofit methods. The curvature ductility demands in the beams and columns in the lower storeys are only slightly reduced by the introduction of the energy dissipating systems.

The distribution of peak horizontal deflections and accelerations along the building height are given in Figure 14 for all analyses performed. Again, the responses of the two energy dissipating systems are nearly identical. The peak displacements are not reduced significantly by the presence of either energy dissipating system. Both retrofit schemes lowered the peak accelerations in the top storeys but caused an increase in acceleration levels in the lower floors. The accelerations in the structure retrofitted with ring-spring devices are higher than the corresponding accelerations in the building with slotted-bolted connections.

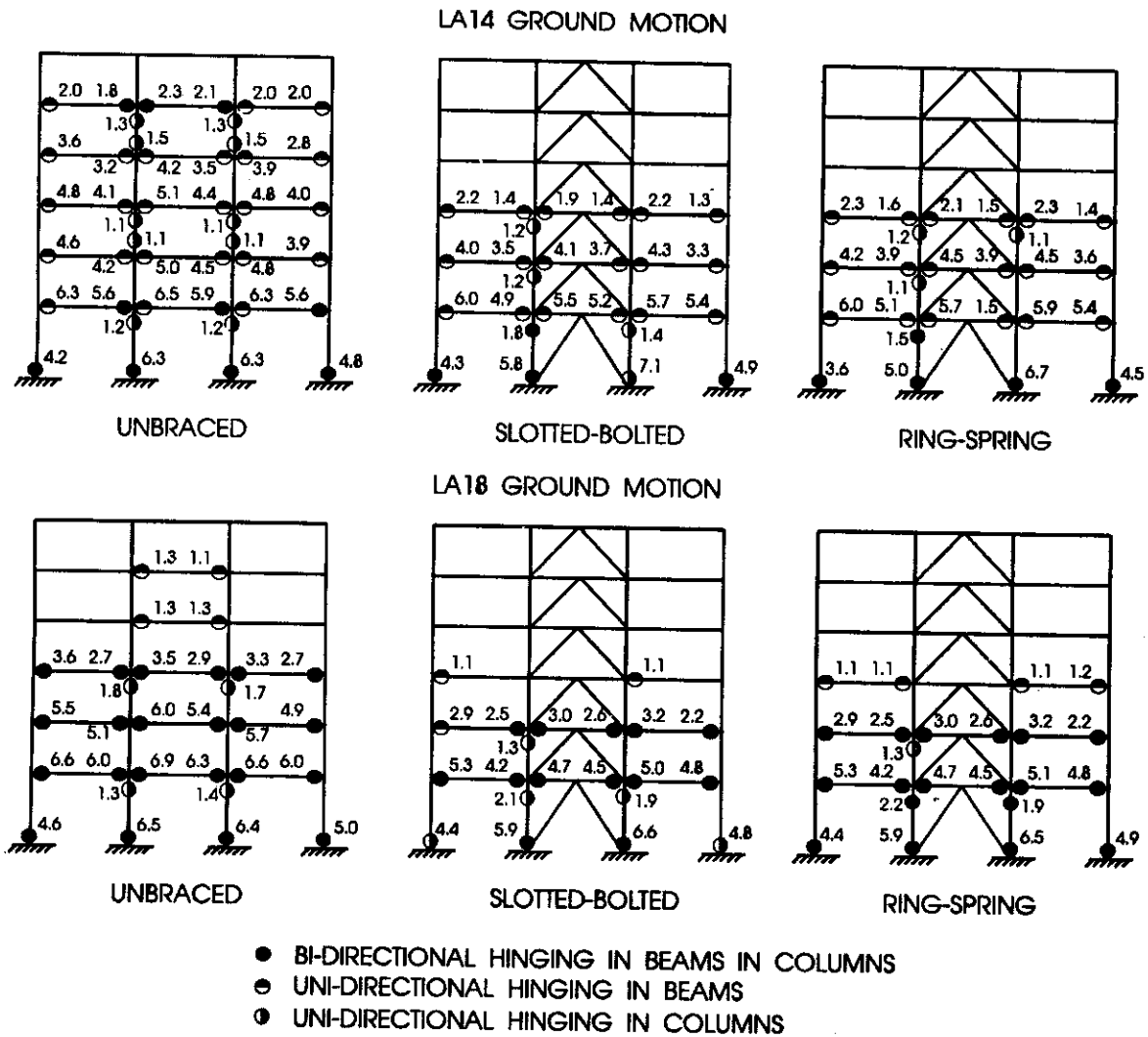


Fig. 13 Plastic hinge distributions, slotted bolted and ring-spring systems, LA14 and LA18 ground motions

The roof residual deflections, computed 5 s after the end of the ground motions, are given in Table 2. For the LA14 ground motion, a significant residual deflection of 84 mm occurs at the roof level when the slotted-bolted friction devices are introduced. The ring-spring system limits the permanent deflections of the structure for both ground motions.

Table 2: Permanent Deflections at Roof Level

Structural Configuration	Permanent Deflection (mm)	
	LA14 Ground Motion	LA18 Ground Motion
Unbraced Frame	54	37
Braced Frame with Slotted-Bolted Connections	84	4
Braced Frame with Ring-Spring Devices	14	9

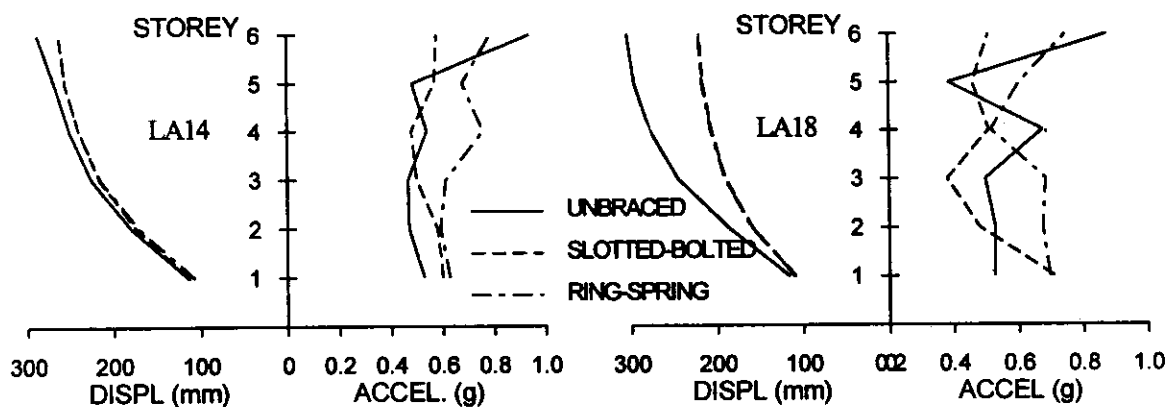


Fig. 14 Distribution of peak deflections and peak accelerations, slotted bolted and ring-spring systems, LA14 and LA18 ground motions

## CONCLUSIONS

The procedure proposed by Filiatrault and Cherry (1990) for determining the optimum slip load of passive friction energy dissipation systems for building moment resisting frames was applied to a six-storey typical steel moment resisting frame. The performance of two friction energy dissipating systems was examined for that building: slotted-bolted system and ring-spring system.

For the slotted-bolted system, three different ground motion ensembles were considered and the amplitude of the slip load was varied. The influence of modifying the vertical distribution of the slip load and the stiffness of the bracing members was also examined. The main conclusions of this investigation are:

- The characteristics of the ground motion ensembles considered in this investigation were significantly different. The near-fault records exhibited higher amplitudes and more severe acceleration pulses than the ground motions of the other two groups. In addition, their energy was concentrated in longer periods. The amplitude of the unscaled El Centro and Taft records was lower than all the other records. Consequently, the response of the building studied and the efficiency of the energy dissipating systems also varied significantly depending upon the ensemble of ground motions.
- Under the unscaled El-Centro and Taft ground motions, the structure remained essentially elastic, regardless of the slip load specified for the energy dissipating system. For these records, the optimum slip load was lower than the value predicted by the proposed method and the use of the friction system permitted to reduce both the inter-storey drifts and absolute accelerations.
- Under the LA and NF ground motions, the unbraced and braced frames underwent significant inelastic response. An optimum slip load nearly equal to the proposed value was clearly identified at the top floor only, both for the inter-storey drift and the absolute acceleration. At the lower levels, the energy dissipating system was less efficient than under the El Centro and Taft records. Its overall performance under the LA records was still satisfactory, however, despite the fact that these ground motions exhibited higher peak accelerations than the value used in the design of the system. When subjected to the NF ground motions, very large inter-storey drifts and large plastic rotation demand developed in beams and columns at the first floor. This response level could not be reduced by increasing the slip load of the slotted-bolted devices. This poor performance is attributed to the impulsive nature of the NF ground motions which does not allow the devices to dissipate the input

energy through cyclic sliding. Instead, the severe acceleration pulses induce large deformations before the building starts to oscillate.

- Increasing the stiffness of the braces or using a linear variation of the slip load over the height of the building, with the larger slip load at the base, slightly improved the response of the braced structure.

The performance of the ring-spring system was compared to that of the slotted-bolted system for two ground motions of the same group. This limited study indicated that both systems prevented the beams and columns in the upper storeys from yielding. The ring-spring system was more efficient than the slotted bolted system in reducing the permanent deflections of the structure. The peak absolute accelerations in the structure retrofitted with ring-spring devices are higher than the corresponding accelerations in the building with slotted-bolted connections.

Further extensive analytical studies are required to fully evaluate the impact of near-fault ground motions on the seismic behaviour of steel moment-resisting structures equipped with passive energy dissipating systems. In particular, the influence of the building height and that of the actual lateral resistance of the unbraced building should be examined. Nevertheless, the results obtained in this study highlight the fact that retrofit of steel structures with friction damping systems must be carefully assessed using non-linear time-history dynamic analyses for the full range of expected ground motion types at the site.

#### ACKNOWLEDGEMENTS

This research was supported by the Natural Sciences and Engineering Research Council of Canada (NSERC) and the "Fonds pour la formation de chercheurs et l'aide à la recherche" (FCAR) of Quebec.

#### REFERENCES

1. AISC (1993). "Load and Resistance Factor Design Specification for Structural Buildings," American Institute of Steel Construction, Inc., Chicago, IL.
2. AISC (1997). "Seismic Provisions for Structural Steel Buildings," American Institute of Steel Construction, Inc., Chicago, IL.
3. Carr, A.J. (1996). "Ruaumoko - Inelastic Dynamic Analysis Program," Department of Civil Engineering, University of Canterbury, Christchurch, New Zealand.
4. Filiatrault, A. and Cherry, S. (1988). "Seismic Design of Friction Damped Braced Steel Plane Frames by Energy Methods," Earthquake Engineering Research Laboratory Report UBC-EERL-88-01, Department of Civil Engineering, University of British Columbia, Vancouver, Canada.
5. Filiatrault, A. and Cherry, S. (1990). "Seismic Design Spectra for Friction-Damped Structures," ASCE, Journal of Structural Engineering, Vol. 116, No. 5, pp. 1334-1355.
6. Grigorian, C.E., Yang, T.S. and Popov, E.P. (1992). "Slotted Bolted Connection Energy Dissipators," Report UCB/EERC-92/10, Earthquake Engineering Research Centre, Univ. of California, Berkeley, CA.
7. Hall, J.F. (1995). "Parameter Study of the Response of Moment -Resisting Steel Frame Buildings to Near-Source Ground Motions," Technical Report SAC95-05: *Parametric Analytical Investigation of Ground Motion and Structural Response, Northridge Earthquake of January 17, 1994*. Sacramento, CA, 1.1-1.83.
8. ICBO (1994). "Uniform Building Code - Vol 2," International Conference of Building Officials, Whittier, CA.
9. Kar, R. and Rainer, J.H. (1995). "Friction-Based Energy Dissipation Unit for Circuit Breaker," Proceedings of the 4<sup>th</sup> U.S. Conference Sponsored by the Technical Council on Lifeline Earthquake Engineering/ASCE, San Francisco, CA, pp. 344-351.
10. Kar, R. and Rainer, J.H. (1996). "New Damper for Seismic Control of Structures," Proceedings of the 1<sup>st</sup> Structural Speciality Conference, Edmonton, Alberta, pp. 835-841.
11. Kar, R., Rainer, J.H. and Lefrançois, A.C. (1996). "Dynamic Properties of a Circuit Breaker with Friction-Based Seismic Dampers," Earthquake Spectra, Vol. 12, No. 2, pp. 297-314.

12. Kar, R., Filiatrault, A. and Tremblay, R. (1998). "Energy Dissipation Device for Seismic Control of Structures," Proceedings 6<sup>th</sup> U.S. Nat. Conference on Earthquake Engineering, Seattle, WA, Paper No. IC-26.
13. Pall, A.S. and Marsh, C. (1982). "Response of Friction Damped Braced Frames," Journal of the Structural Division, ASCE, Vol. 108, pp. 1313-1323.
14. SAC Joint Venture (1995). "Characterization of Ground Motions During the Northridge Earthquake of January 17, 1994," Technical Report SAC95-03, Sacramento, CA.
15. SAC Joint Venture (1997). "Develop Suites of Time Histories," Project Task: 5.4.1, Draft Report, Sacramento, CA.
16. SEAOC (1996). "Recommended Lateral Force Requirements and Commentary, Appendix B – Vision 2000, Conceptual Framework for Performance-Based Seismic Design," Seismology Committee, Structural Engineers Association of California.
17. Shepherd, R. and Erasmus, L.A. (1988). "Ring Spring Energy Dissipators in Seismic Resistant Structures," Proceedings of the 9<sup>th</sup> World Conference on Earthquake Engineering, Tokyo-Kyoto, Japan, V-767/V-772.
18. Tremblay, R. and Stierner, S., (1993). "Energy Dissipation Through Friction Bolted Connections in Concentrically Braced Steel Frames," Proceedings of the ATC-17-1 Seminar on Seismic Isolation, Passive Energy Dissipation, and Active Control, San Francisco, CA. II: 557-568.
19. Tsai, K.C. and Popov, E.P. (1988). "Steel Beam-Column Joints in Seismic Moment Resisting Frames," Report No. UCB/EERC-88/19, Earthquake Engineering Research Center, University of California, Berkeley, CA.